Supported by Office of Science U.S. DEPARTMENT OF ENERGY

Resistive Wall Mode Active Control Physics Design for KSTAR*

Y.S. Park[1], S.A. Sabbagh[1], J.G. Bak[2], J.M. Bialek[1], J.W. Berkery[1], S.G. Lee[2], Y.M. Jeon[2], W.H. Ko[2], Y.K. Oh[2]

[1]Department of Applied Physics, Columbia University, New York, NY
[2]National Fusion Research Institute, Daejeon, Korea

presented at the
18th Workshop on MHD Stability Control
November 18 - 20, 2013
Santa Fe, NM

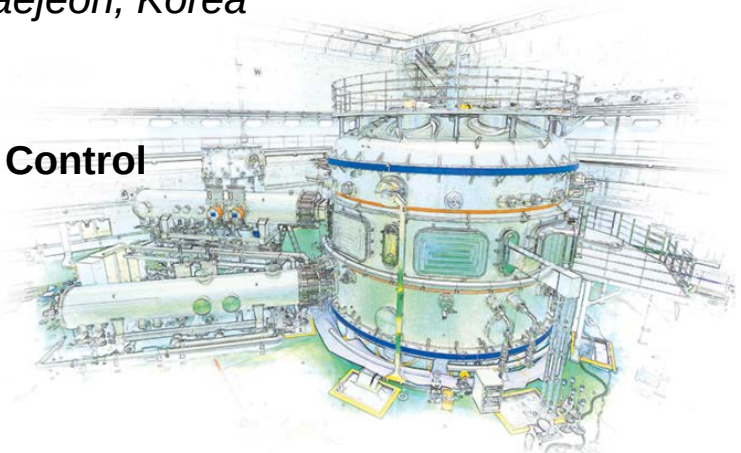

V1.1

In collaboration with NFRI National Fusion Research Institute

*Work supported by the U.S. Department of Energy under contract DE-FG02-99ER54524.

RWM stabilization projection is an urgent need for KSTAR

- Understanding and maintenance of MHD stability at high β_N over long pulse duration are key KSTAR, ITER goals
  - Altering plasma rotation to study MHD stability, and to operate in most ITER relevant low rotation regime are key
- Outline
  - High β_N results exceeding the n = 1 ideal no-wall limit
  - Open loop control of plasma rotation using 3D fields
  - RWM control performance calculations using KSTAR control hardware and control improvement by optimized 3D sensors

First plasmas exceeding $\beta_N > \beta_N^{no\text{-}wall}$ mark initial KSTAR advanced tokamak operation

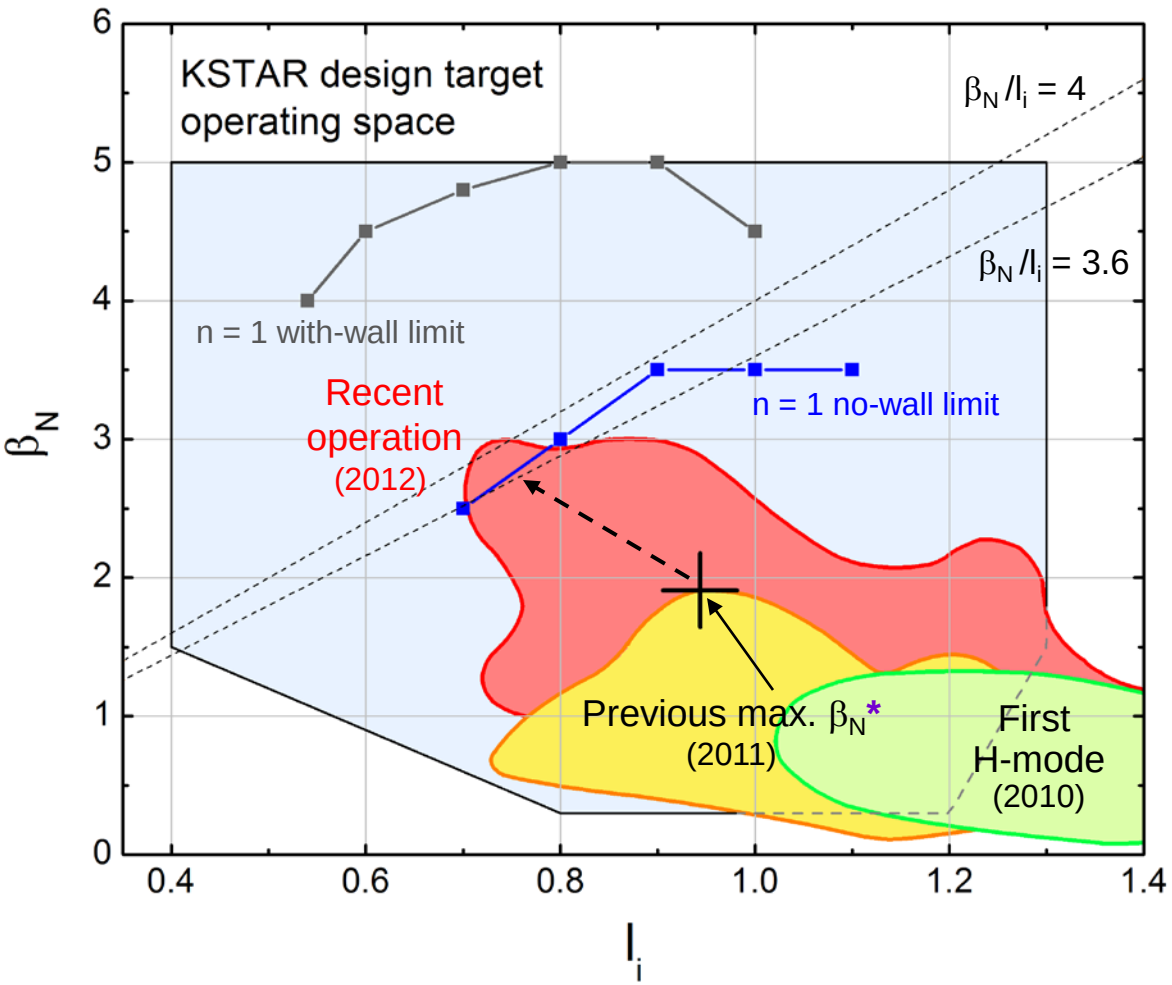

Normalized beta vs. internal inductance from EFIT reconstruction

- I_p scan performed to determine "optimal" β_N vs. I_p
  - B_T in range 1.3 - 1.5 T
  - β_N up to 2.9
- $\beta_N/l_i > 3.6$ (80% increase from 2011)
  - A high value for advanced tokamaks
- Mode stability
  - Target plasma is at published computed ideal n = 1 no-wall stability limit** (DCON)
  - Plasma is subject to RWM instability, depending on plasma rotation profile
  - Rotating n = 1, 2 mode activity observed in core during H-mode

*Y.S. Park, et al., Nucl. Fusion **53** (2013) 083029

** O. Katsuro-Hopkins, et al., Nucl. Fusion **50** (2010) 025019

n = 2 non-axisymmetric field used to alter plasma rotation profile non-resonantly in using in-vessel control coil

- Test plasma characteristics vs. toroidal rotation by slowing plasma with non resonant n = 2 NTV using IVCC

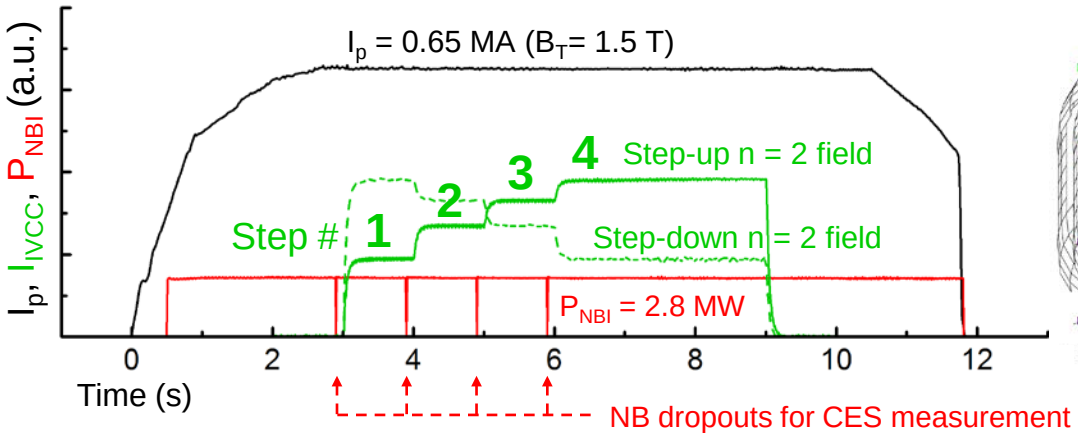

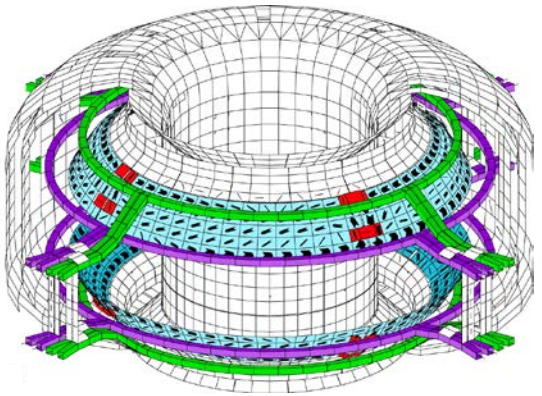

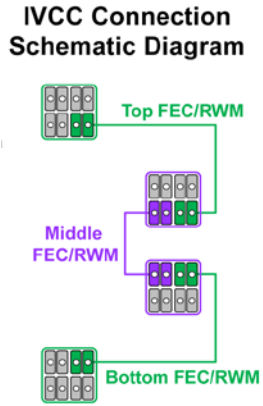

KSTAR in-vessel control coil (IVCC)

Simplified expression of NTV force ("1/ν regime")

$$\left\langle \hat{e}_t \bullet \vec{\nabla} \bullet \overleftrightarrow{\Pi} \right\rangle_{(1/\nu)} = B_t R \left\langle \frac{1}{B_t} \right\rangle \left\langle \frac{1}{R^2} \right\rangle \frac{\lambda_{1i} p_i}{\pi^{3/2} \nu_i} \varepsilon^{3/2} (\omega_\phi - \omega_{NC}) I_\lambda$$

K.C. Shaing, et al.,
PPCF **51** (2009) 035004

$T_i^{5/2}$

Inverse aspect ratio

Steady-state velocity

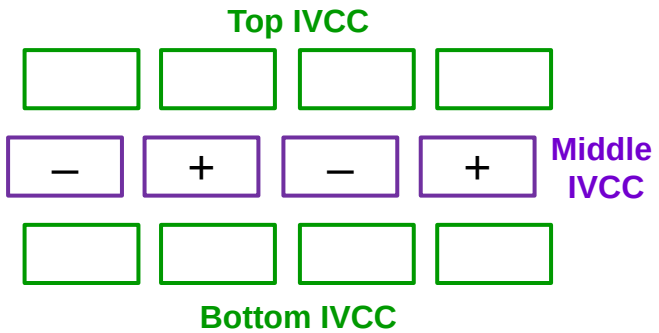

Applied n = 2 even parity configuration

- Pre-requisite for study of NTV physics in KSTAR – comparison to NSTX (low A.R.)

Changing the in-vessel control coil current in steps altered rotation in a controlled fashion without hysteresis

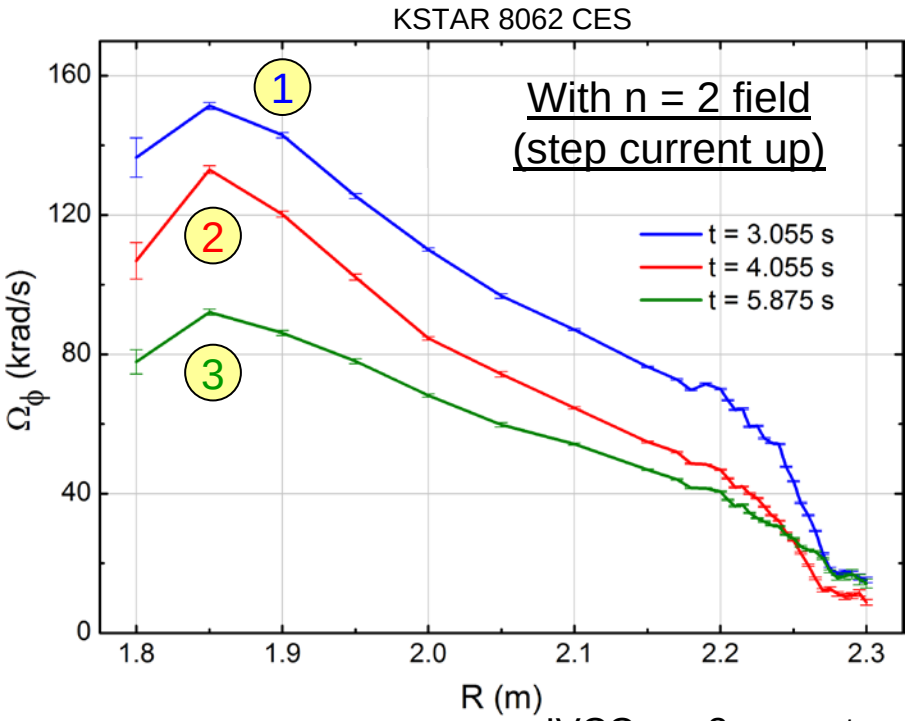

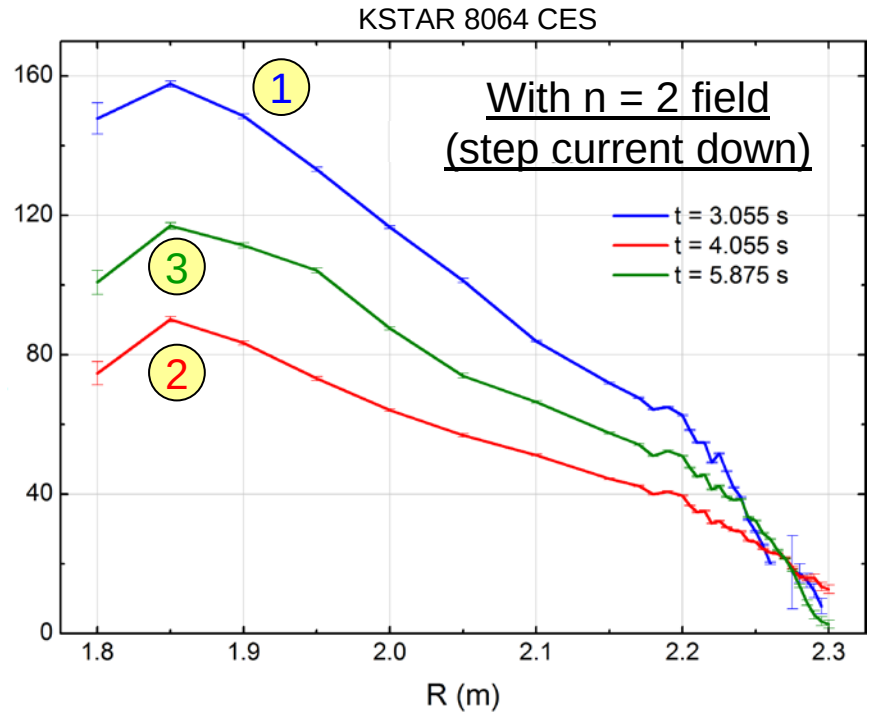

IVCC n = 2 current

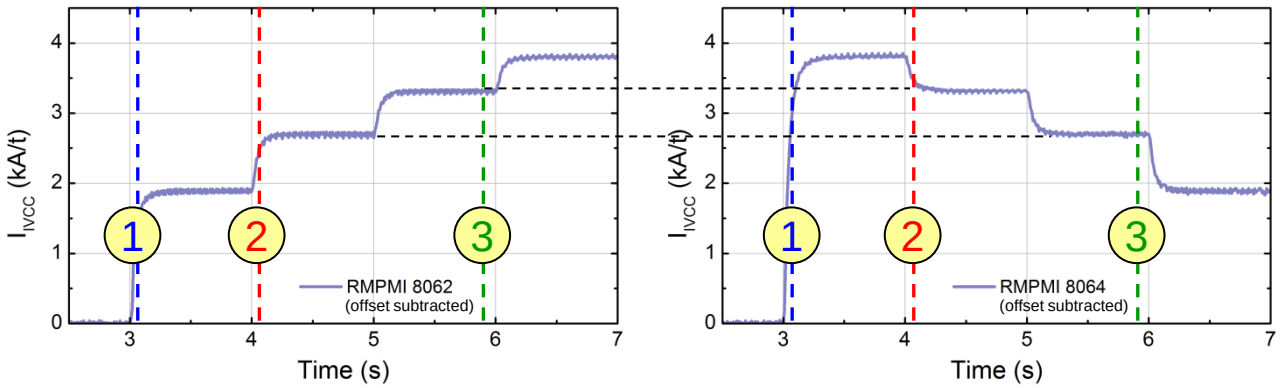

- At same IVCC current, rotation level is very similar without hysteresis - important for control

Change in the measured steady-state rotation profile is analyzed by torque balance

- Torque balance relation in steady-state

$$\frac{d(I\Omega_\phi)}{dt} = T_{NBI} + T_D + T_{NTV} + T_{J\times B} = 0$$

No existing tearing mode

NBI torque — Momentum diffusion — NTV torque

- Equation in flux coordinate (i = ion)

$$n_i m_i \left\langle R^2 \right\rangle \frac{\partial \Omega_\phi}{\partial t} + \Omega_\phi \left\langle R^2 \right\rangle m_i \frac{\partial n_i}{\partial t} + n_i m_i \Omega_\phi \frac{\partial \left\langle R^2 \right\rangle}{\partial t} +$$

$$n_i m_i \left\langle R^2 \right\rangle \Omega_\phi \left(\frac{\partial V}{\partial \Psi_N} \right)^{-1} \frac{\partial}{\partial t} \left(\frac{\partial V}{\partial \Psi_N} \right) =$$

$$\left(\frac{\partial V}{\partial \Psi_N} \right)^{-1} \frac{\partial}{\partial \Psi_N} \left(\frac{\partial V}{\partial \Psi_N} n_i m_i \chi_\phi \left\langle R^2 (\nabla \Psi_N)^2 \right\rangle \frac{\partial \Omega_\phi}{\partial \Psi_N} \right) + \sum T_{\text{torque}}$$

(V = volume, χ_ϕ = toroidal momentum diffusivity)

by assuming

$$\frac{\partial n_i}{\partial t} = \frac{\partial \left\langle R^2 \right\rangle}{\partial t} = \frac{\partial}{\partial t} \left(\frac{\partial V}{\partial \Psi_N} \right) = 0$$ then the equation reduces to

$$n_i m_i \left\langle R^2 \right\rangle \frac{\partial \Omega_\phi}{\partial t} = \left(\frac{\partial V}{\partial \Psi_N} \right)^{-1} \frac{\partial}{\partial \Psi_N} \left(\frac{\partial V}{\partial \Psi_N} n_i m_i \chi_\phi \left\langle R^2 (\nabla \Psi_N)^2 \right\rangle \frac{\partial \Omega_\phi}{\partial \Psi_N} \right) + T_{NBI} + T_{NTV}$$

$\Omega_\phi \approx$ constant at each n = 2 current step

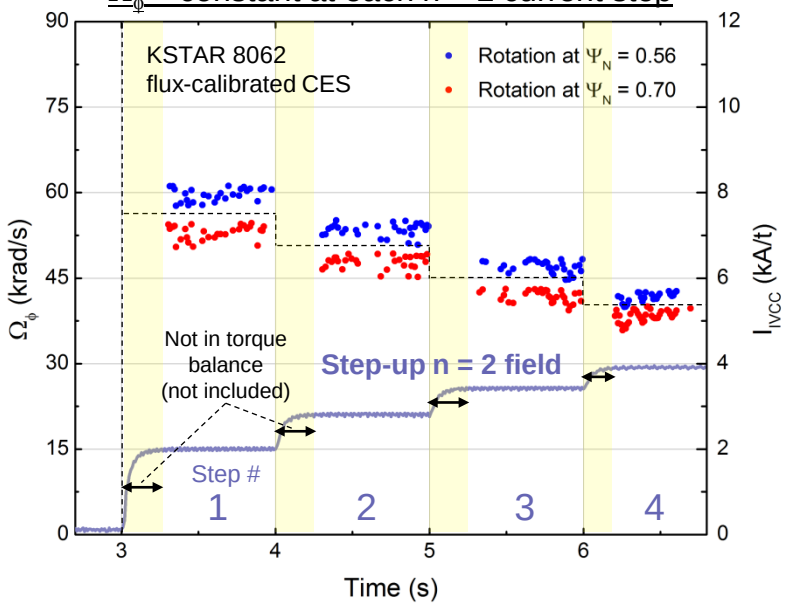

- Since the plasma boundary is not stationary, rotation at constant normalized flux surface is computed by using high time resolution EFIT flux grid at every time point shown

Reduced formulation of the steady-state torque balance problem

- In steady-state profiles $\left(\frac{\partial \Omega_\phi}{\partial t} = 0\right)$,

$$0 = \left(\frac{\partial V}{\partial \Psi_N}\right)^{-1} \frac{\partial}{\partial \Psi_N}\left(\frac{\partial V}{\partial \Psi_N} n_i m_i \chi_\phi \left\langle R^2 (\nabla \Psi_N)^2 \right\rangle \frac{\partial \Omega_\phi}{\partial \Psi_N}\right) + T_{NBI} + T_{NTV}$$

$$0 = \mathrm{C1} \frac{\partial}{\partial \Psi_N}\left(\mathrm{C2} \frac{\partial \Omega_\phi}{\partial \Psi_N}\right) + T_{NBI} + T_{NTV} \quad \rightarrow \quad 0 = \mathrm{C3} \frac{\partial \Omega_\phi}{\partial \Psi_N} + \mathrm{C4} \frac{\partial^2 \Omega_\phi}{\partial \Psi_N^2} + T_{NBI} + T_{NTV}$$

Express T_{NTV} as non-resonant (damping scales with Ω_ϕ)

$T_{NTV} = K\, \Omega_\phi\, \delta B^P$ (K = function of T_i) (Resonant field amplification is insignificant as $\beta_N < \beta_N^{\text{no-wall}}$)

$T_{NBI} = \text{constant}$

C3, C4 are assumed to be constant over time at fixed flux surface, then by taking difference of the equation between steady-state NTV steps,

$$K\left(\Omega_\phi\, \delta B^P\Big|_{j2} - \Omega_\phi\, \delta B^P\Big|_{j1}\right) = \mathrm{C5}\left(\frac{\partial \Omega_\phi}{\partial \Psi_N}\Big|_{j2} - \frac{\partial \Omega_\phi}{\partial \Psi_N}\Big|_{j1}\right) + \mathrm{C6}\left(\frac{\partial^2 \Omega_\phi}{\partial \Psi_N^2}\Big|_{j2} - \frac{\partial^2 \Omega_\phi}{\partial \Psi_N^2}\Big|_{j1}\right)$$

(j = steady-state step #)

with $\delta B \propto I_{IVCC}$ and $\Omega_\phi,\ \frac{\partial \Omega_\phi}{\partial \Psi_N},\ \frac{\partial^2 \Omega_\phi}{\partial \Psi_N^2}$ from flux-calibrated CES profiles

Change in rotation profile gradient by applied n = 2

- Analysis of increasing n = 2 current steps (shot 8062)
  - At constant normalized flux surface, profiles having similar $<n_e>$ and T_i between comparing steady-state steps are chosen in accordance with assumptions

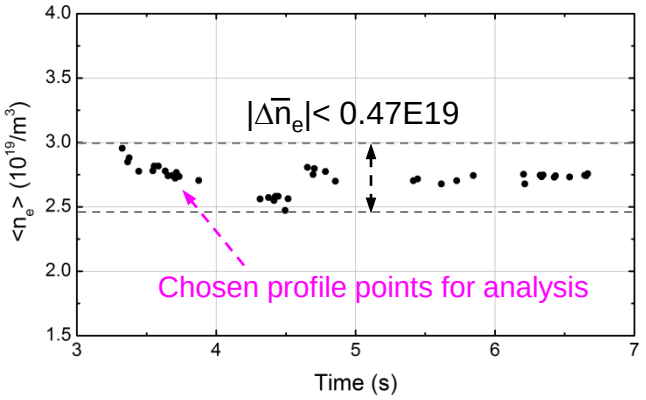

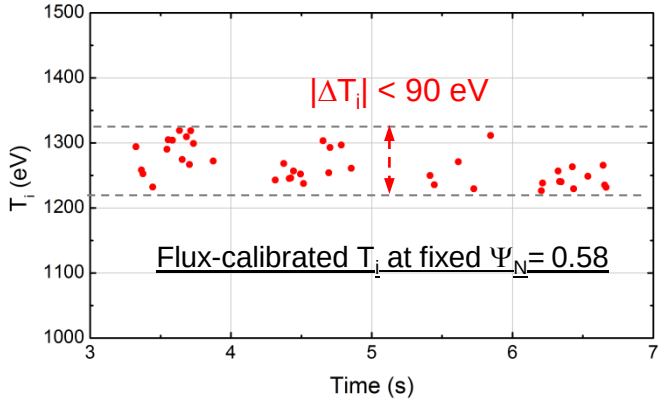

  - Rotation gradient change calculated from measured profiles

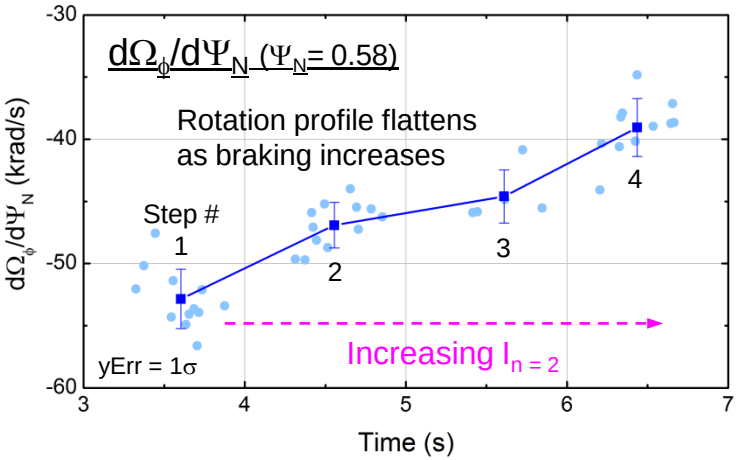

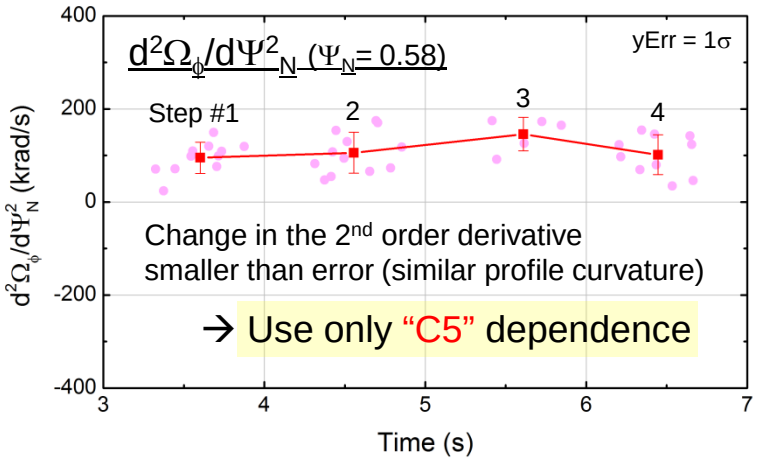

Steady-state profile analysis to examine NTV dependence on δB

- Resulting NTV correlation with different power in δB^P

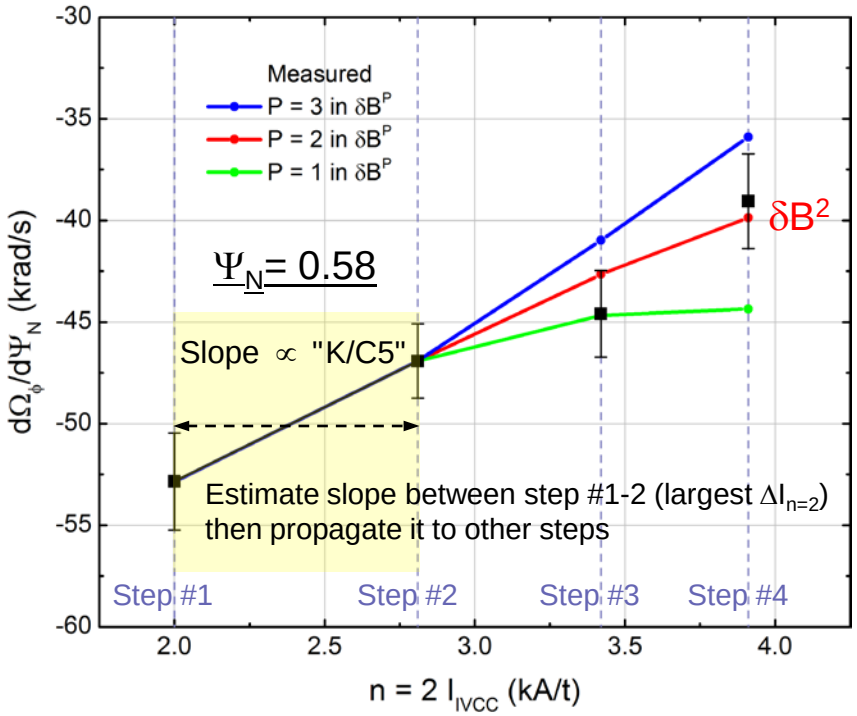

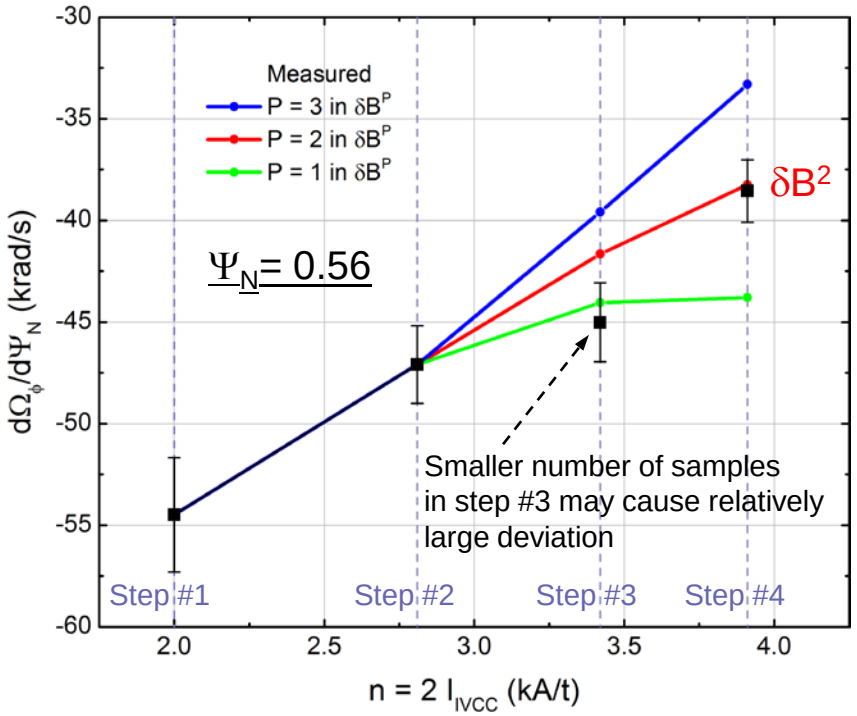

- For the different normalized flux surfaces, T_{NTV} scales well with δB^2

$$T_{NTV-(1/\nu)} \propto \delta B^2 \, T_i^{5/2}$$

Reduced rotation braking correlates with lower T_i

- Analysis of increasing n = 2 current steps with lower T_i (shot 9199)
  - Chosen profiles have $|\Delta T_i| < 50$ eV

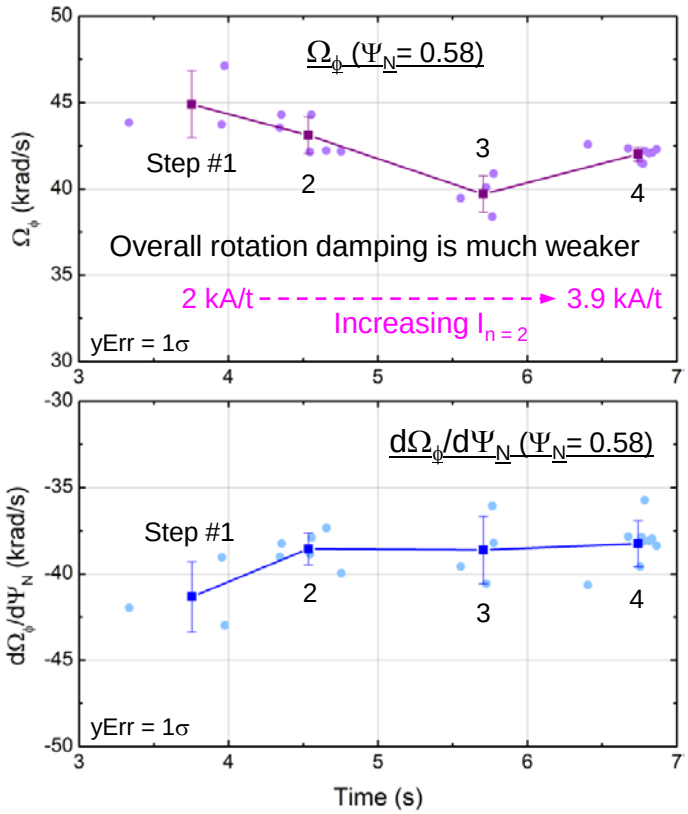

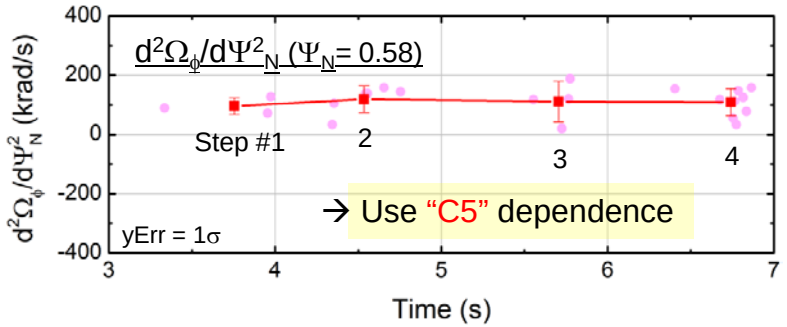

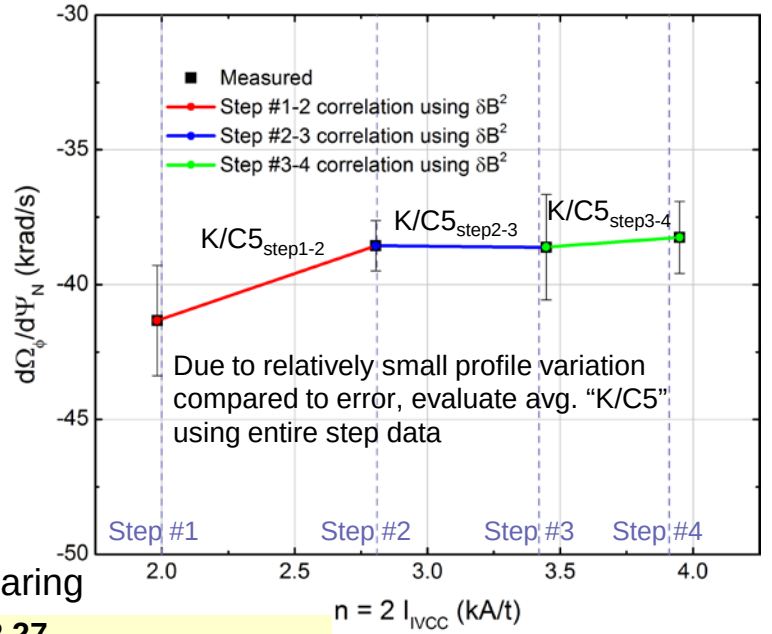

- By assuming the same $C5_{\Psi_N=0.58}$ between two comparing shots,

$$\frac{K^{8062}_{\Psi_N=0.58}}{K^{9199}_{\Psi_N=0.58}} = 6.02 = \left(\frac{T^{8062}_{i,\Psi_N=0.58}}{T^{9199}_{i,\Psi_N=0.58}} = \frac{1262\ \text{eV}}{573\ \text{eV}} \right)^{2.27} \approx T_{NTV-(1/\upsilon)} \propto T_i^{2.5}$$

Active n = 1 RWM control performance determined with 3D sensors

KSTAR RWM control system in VALEN-3D

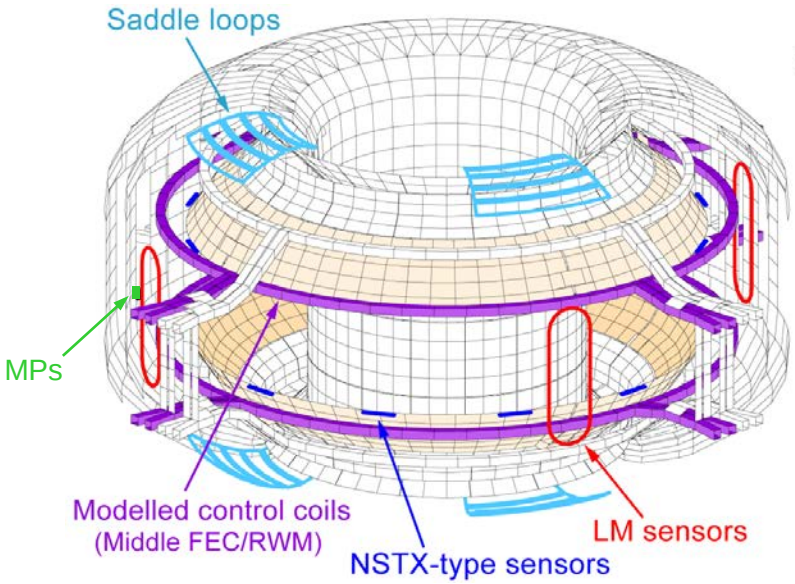

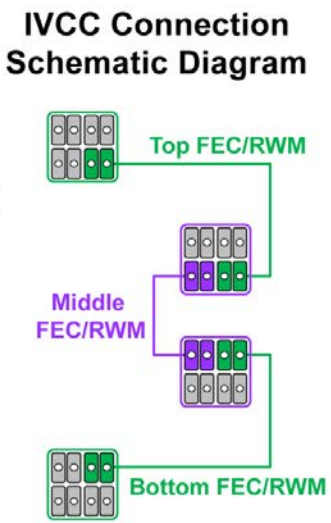

Input n = 1 unstable eigenmode from DCON

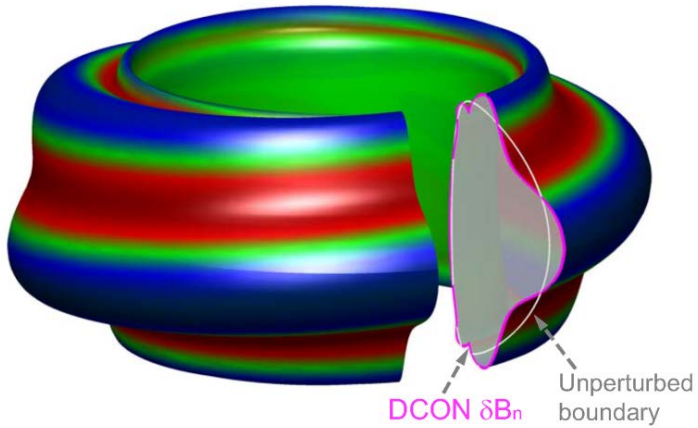

Y.S. Park, et al., Phys. Plasmas submitted

- RWM active control analysis using the KSTAR device sensors
  - n = 1 unstable eigenfunction from DCON (β_N = 5.0, l_i = 0.7 projected equilibrium with H-mode pressure profiles) are used as an input
  - Sensors presently available : 4 midplane LM sensors (90^o toroidally separated) and 40 off-axis SL sensors (10 poloidal positions for the same 4 toroidal positions of the LMs) and MPs

Control coil-induced vessel current significantly limits performance of the LM sensors

(a)

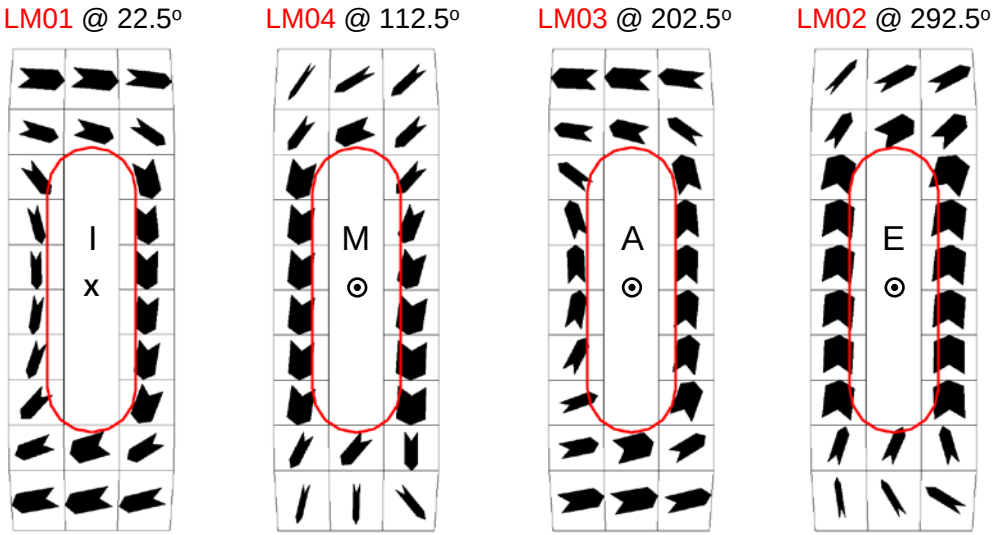

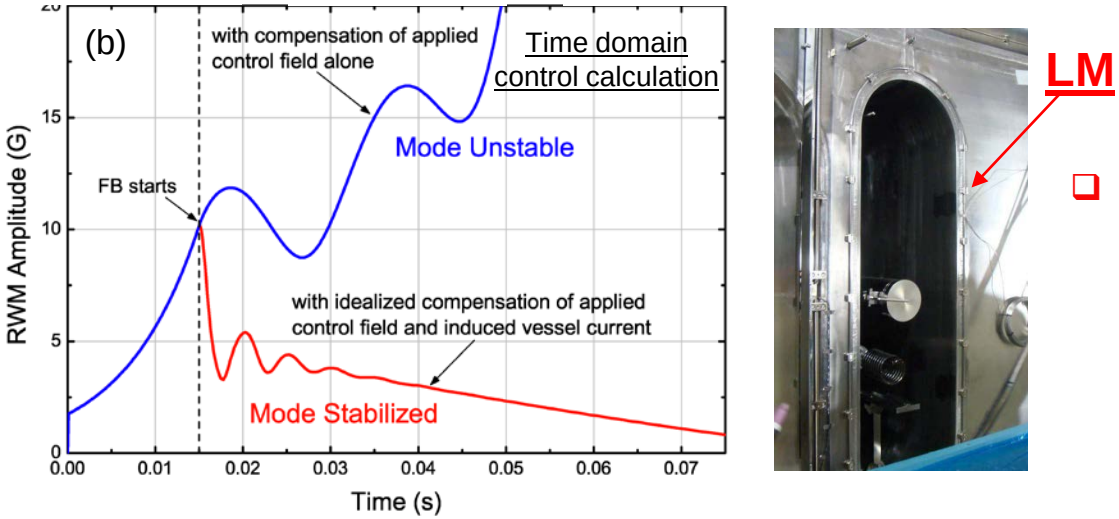

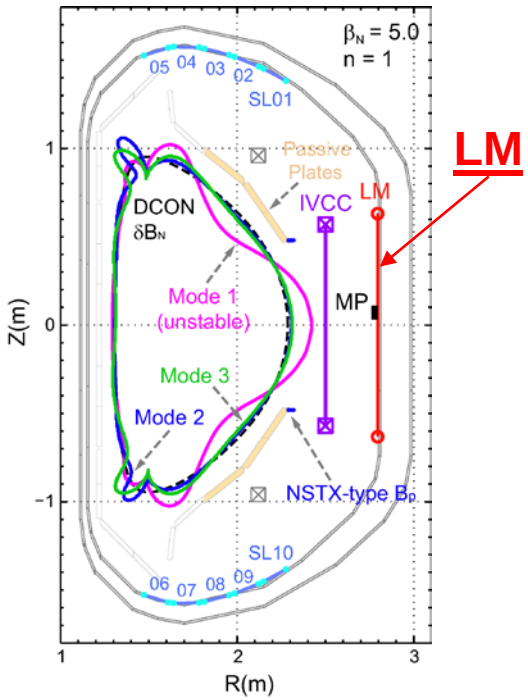

- Effect of vessel current to LMs
  - Control is limited by control coil-induced vessel currents circulating around the elongated port penetrations
  - Induced vessel currents significantly alters the measured mode phase

(a) Induced vessel current during n = 1 feedback
(b) Feedback w/ and w/o compensation of vessel current from LMs

RWM control performance using the LM sensors

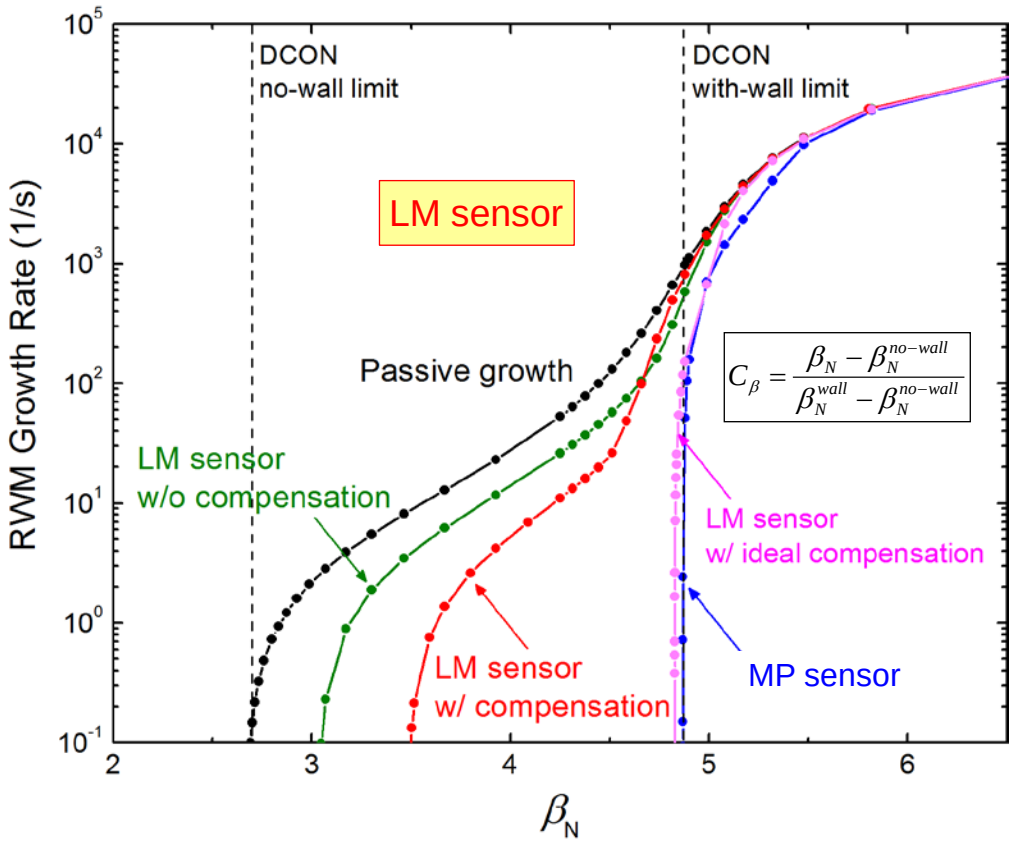

RWM growth rate vs. β_N with feedback using the LM sensors

- Feedback using the LM sensors
  - MP sensors have lowest coupling to vessel/plates: but only 3 toroidal positions, small effective area (blue)
  - Without compensation of external fields, a limited performance C_β = 16% (β_N up to 3.0) can be achieved (green)
  - The applied control field compensation from the sensors increased C_β to 37% (β_N = 3.5) (red)
  - Theoretically performed ideal compensation of the vessel current results in higher C_β = 98% close to the with-wall limit (magenta)

SL sensor performance mostly set by interference due to passive plates

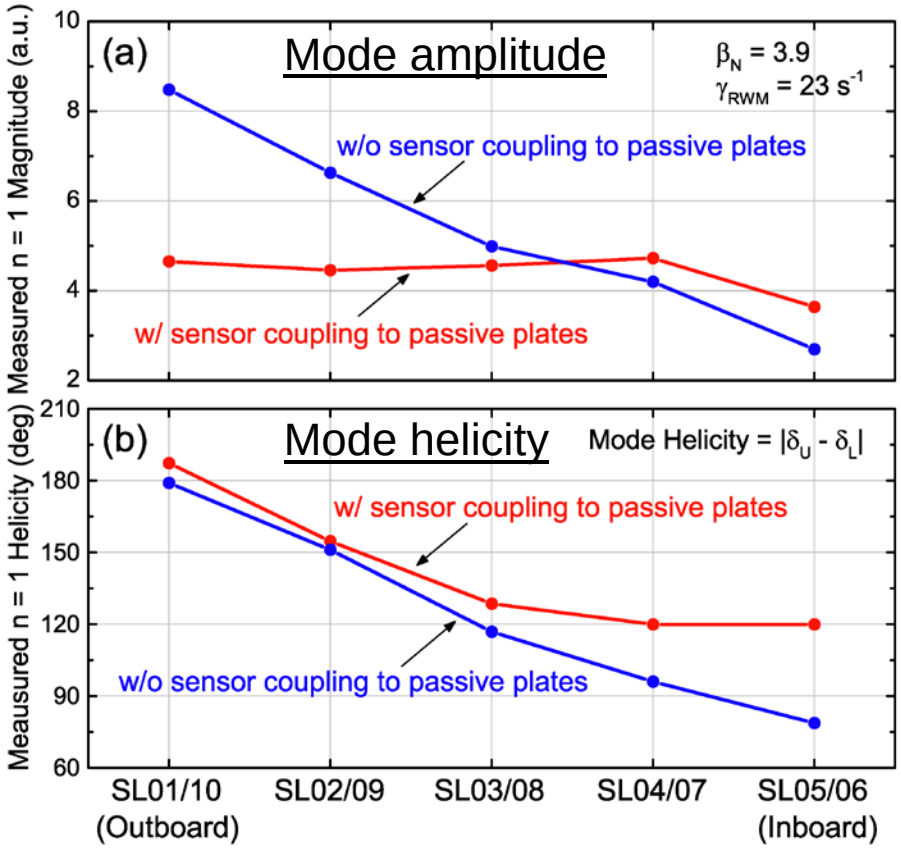

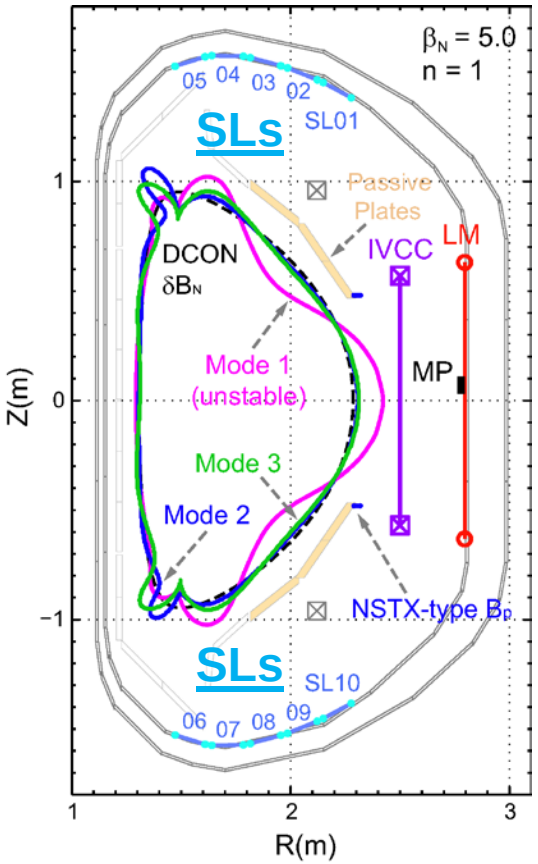

- Effectiveness of the SLs in the presence of passive plates
  - Magnitude of mode perturbation shielding is higher toward the outer SLs
  - However, mode helicity change is significant towards the inner SLs
    → makes successful feedback more difficult

The SL sensors show higher control performance over the LMs

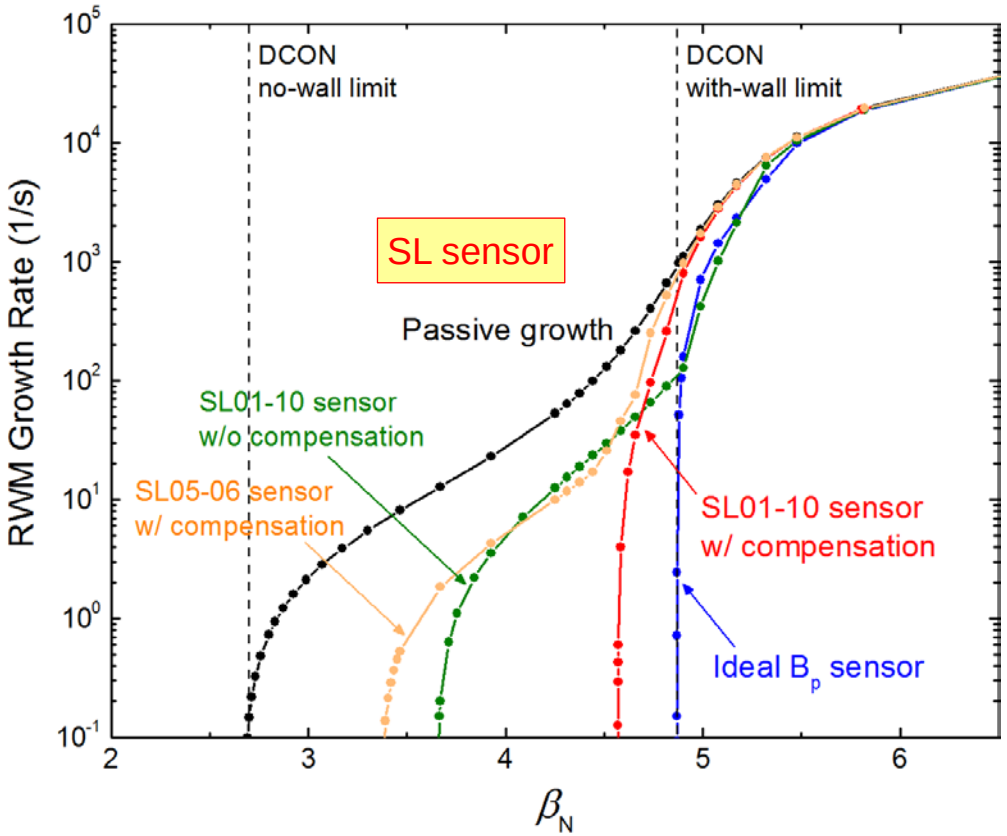

RWM growth rate vs. β_N with different SL sensor configurations

- Performance of two up-down SL sensor pairs
  - Unlike the LMs, vessel current near the SLs does not strongly affect the control performance
  - Compensation of the applied control field alone can increase the C_β from 44% to 86% for the SL01/10 sensors (green) → (red : highest performance among the SLs)
  - Magnitude of mode field measured by the SLs (~2% of the ideal sensor measurement)

Estimation of RWM control power requirements

- Time domain RWM active control calculation to estimate required control power
  - The applied control field compensated SL01/10 (total 8) sensors as mode detection sensors
  - Feedback starts when mode amplitude becomes 10 G (target unstable eigenfunction with β_N = 4.5) with ideal control system assumption (w/o noise and control time delay)
  - Resulting ideal power requirements : P_{RMS} = 136 W, P_{peak} = 282 W, f_{vol} = 30 Hz, I_{peak} = 312 A-turn, V_{peak} = 0.54 V/turn, Δt = 114 ms

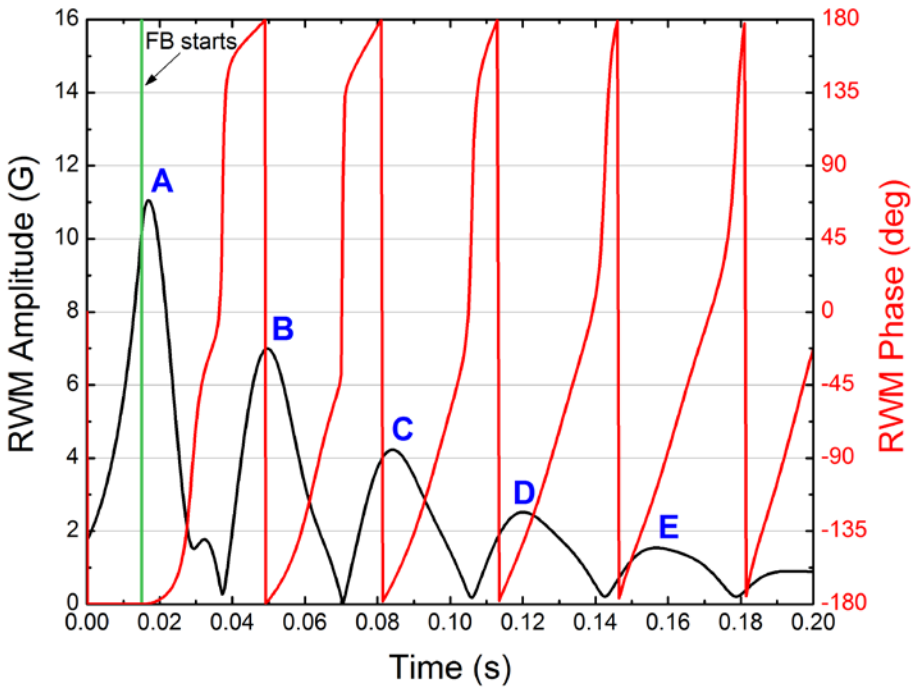

RWM amplitude and phase during feedback

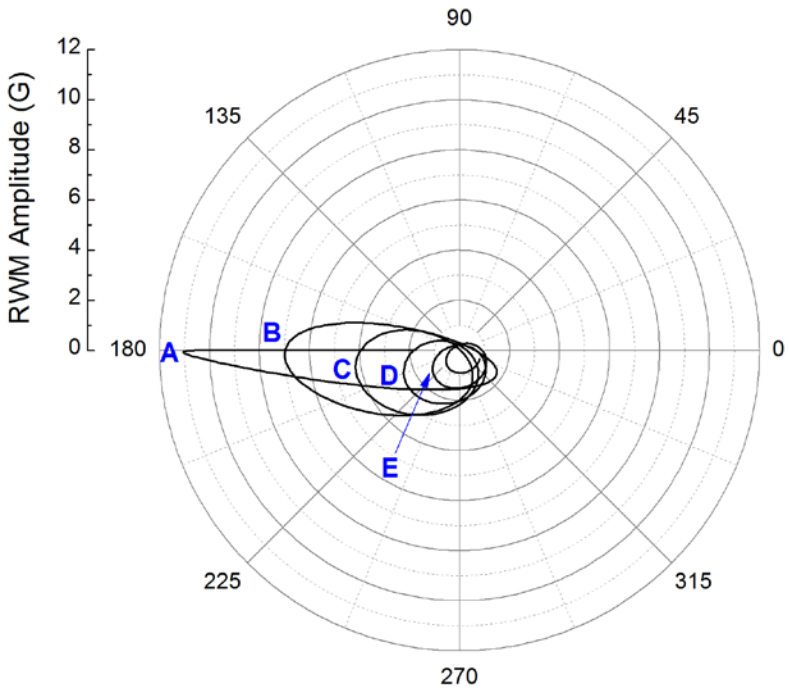

Polar plot

RWM control power dependence on β_N and sensor noise level

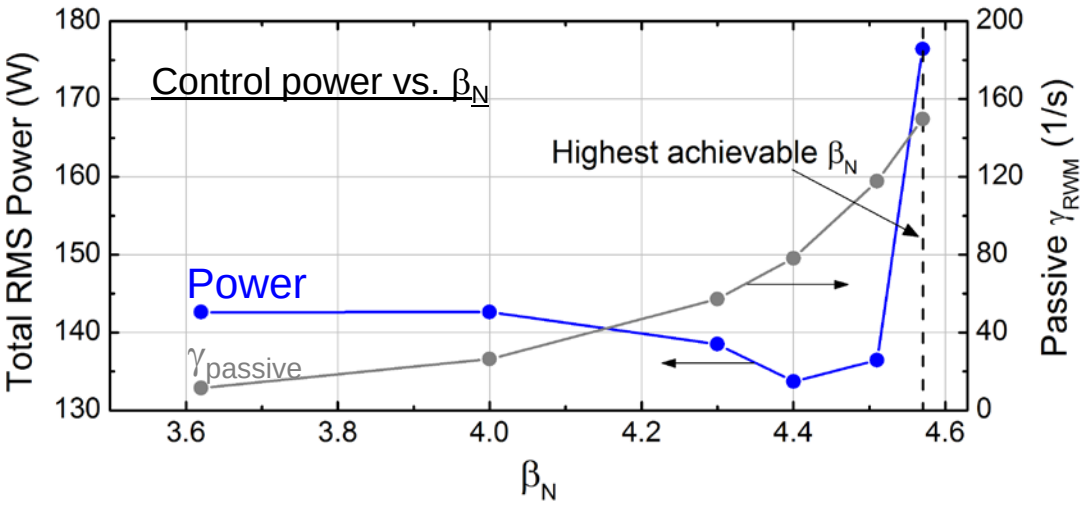

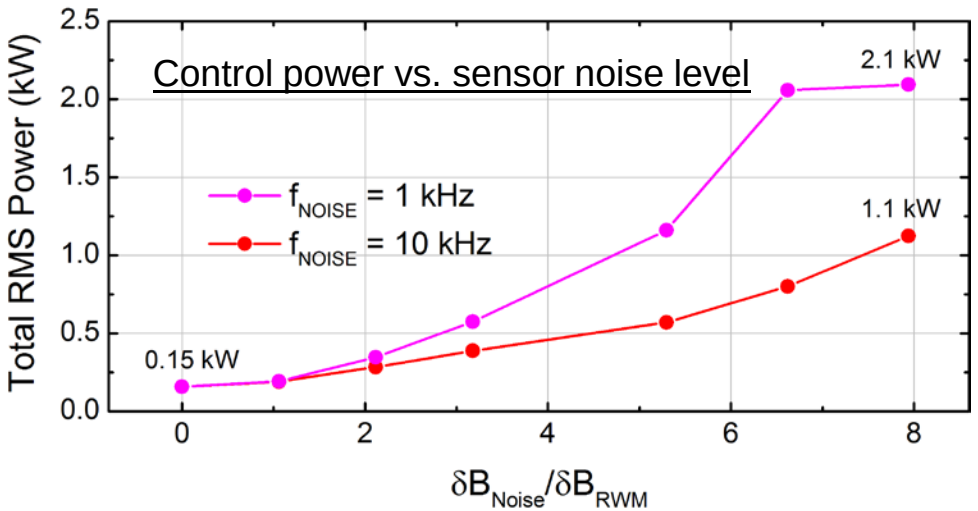

- Control power vs. β_N
  - Control power rapidly increases as β_N approaches the control limit
  - Resulting control time interval : 51 – 131 ms (mode amp. < 2 G)
- Control power vs. sensor noise
  - Required control power increases with increasing sensor noise level
  - Control power increase is significant with lower frequency noise

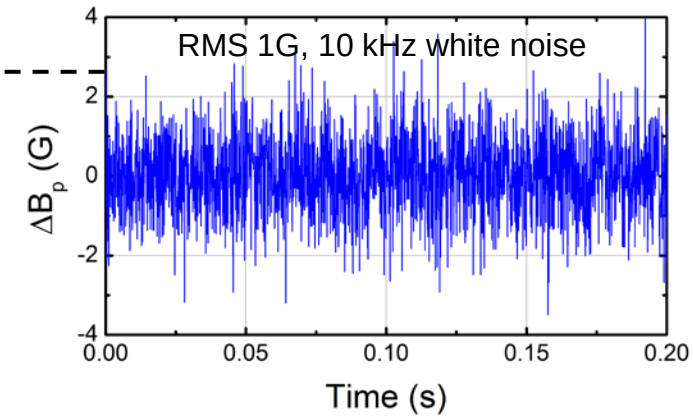

Optimized 3D sensors show higher control performance over the device sensors

NSTX RWM control system

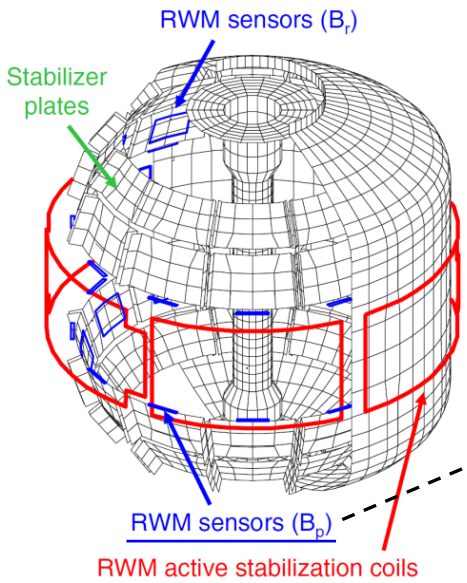

KSTAR

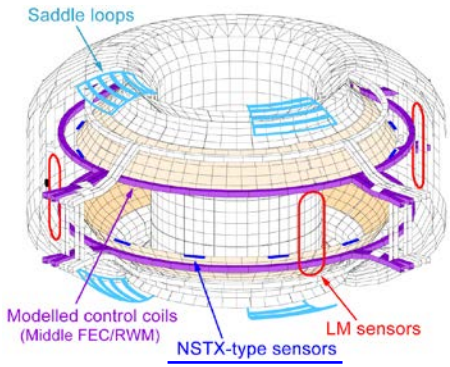

* S.A. Sabbagh, et al., Nucl. Fusion **50** (2010) 025020

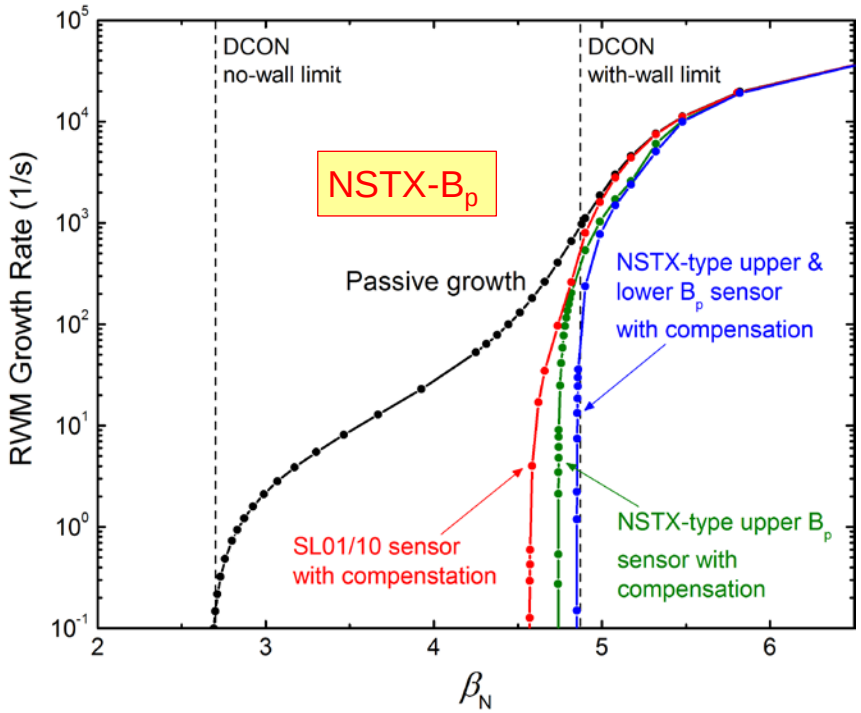

- A new RWM sensor design considered in the KSTAR VALEN model
  - Other sensor sets should be prepared to overcome the confirmed control limitations set by the present device sensors
  - Need more toroidal sensor positions, smallest coupling to applied fields & eddy currents
  - "NSTX-type B_p" sensor performance only weakly affected by vessel and passive plate currents and exhibits improved control performance ($C_{\beta\ SL01/10}$ = 86% → $C_{\beta\ NSTX\text{-}B_p}$ = 99%)

Conclusions

- KSTAR plasmas have exceeded the predicted ideal n = 1 no-wall limit
  - High values of β_N up to 2.9 with $\beta_N / l_i > 3.6$ ($\beta_N^{\text{no-wall}} = 2.5$)
- Plasma toroidal rotation alteration by n = 2 applied field
  - At achieved high normalized beta plasmas, plasma rotation has been significantly reduced (50%) by applied n = 2 field without mode locking
  - Rotation profile alteration by n = 2 fields shows non-resonant braking scales as "1/ν" regime in the NTV theory ($T_{NTV} \sim \delta B^2 T_i^{5/2}$)
- RWM active feedback control analysis using device sensors
  - LM sensors measuring the radial field component of the RWM are strongly affected by vessel currents which result in a limited control performance
  - SL01/10 sensors with applied field compensation perform best, but a low RWM amplitude measured at the off-axis region can produce a low signal-to-noise ratio
  - The optimized 3D sensors motivated by the NSTX-B_p sensors show a clear advantage in control performance
- KSTAR is expected to produce a higher β_N by increased P_{NBI} from 2014

Backup Slides

Experiment to reach and surpass n = 1 no-wall limit in KSTAR planned since 2010

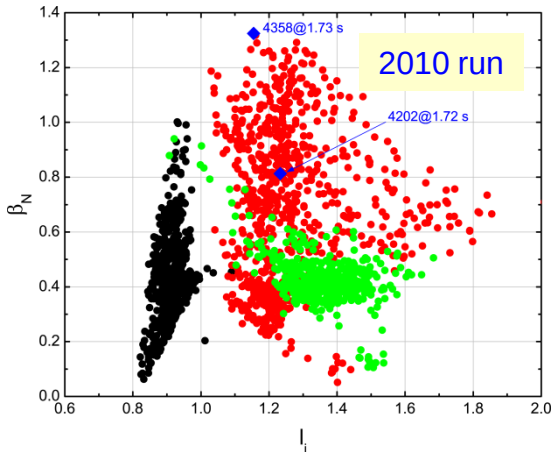

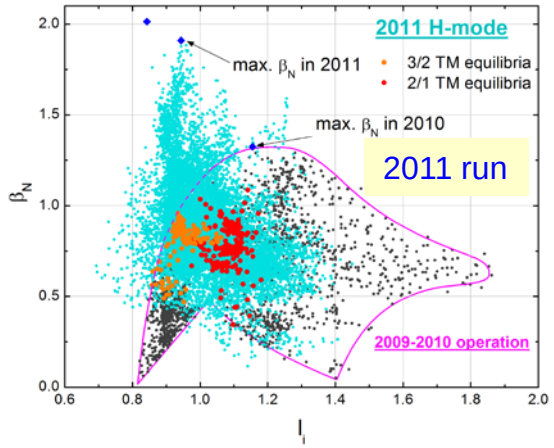

Y.S. Park, et al., Nucl. Fusion **51** (2011) 053001
Y.S. Park, et al., Nucl. Fusion **53** (2013) 083029

Projected n = 1 ideal stability for KSTAR H-mode plasmas

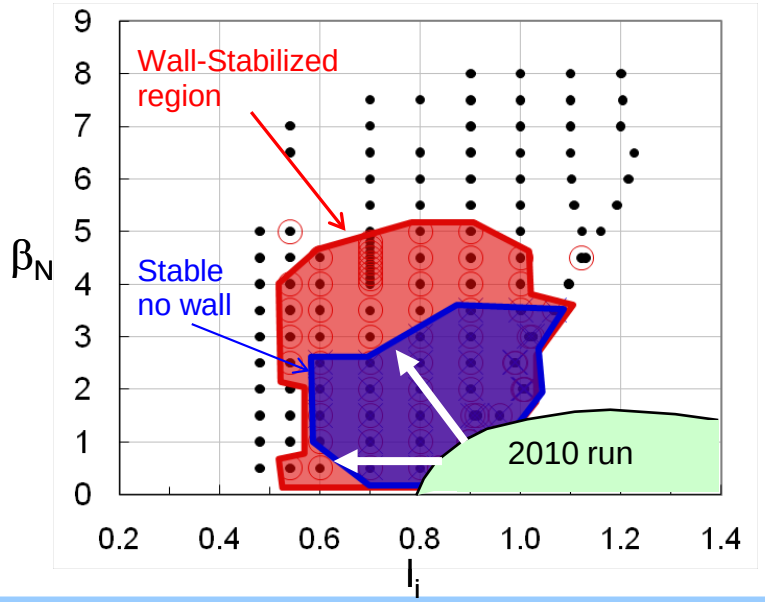

O. Katsuro-Hopkins, et al., NF **50** (2010) 025019

Profiles used in ideal MHD no-wall limit study

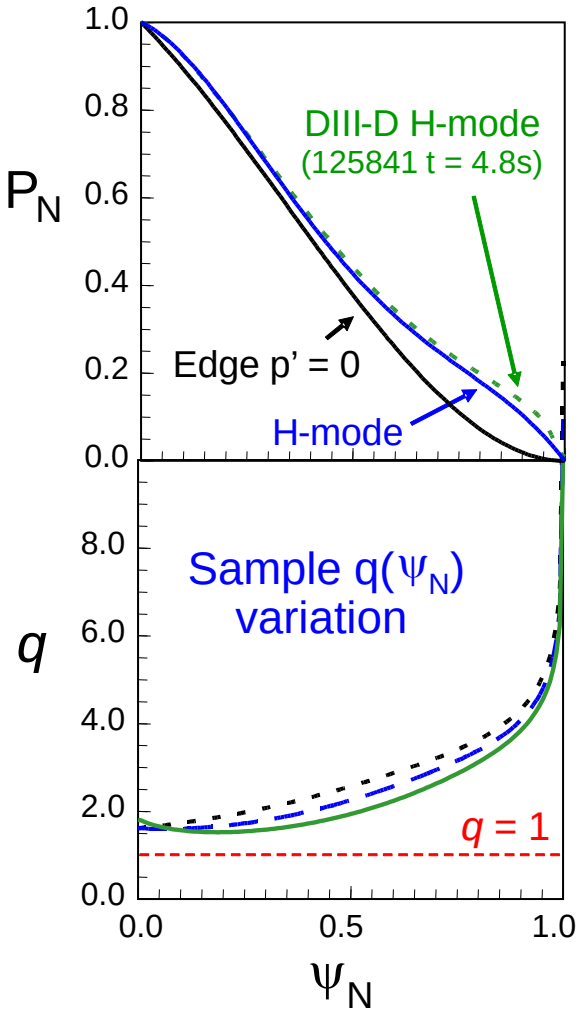

Effect of step increase in n = 2 field observed in mode frequency and x-ray crystal spectrometer rotation data

No IVCC n > 0 field

With IVCC n = 2 field

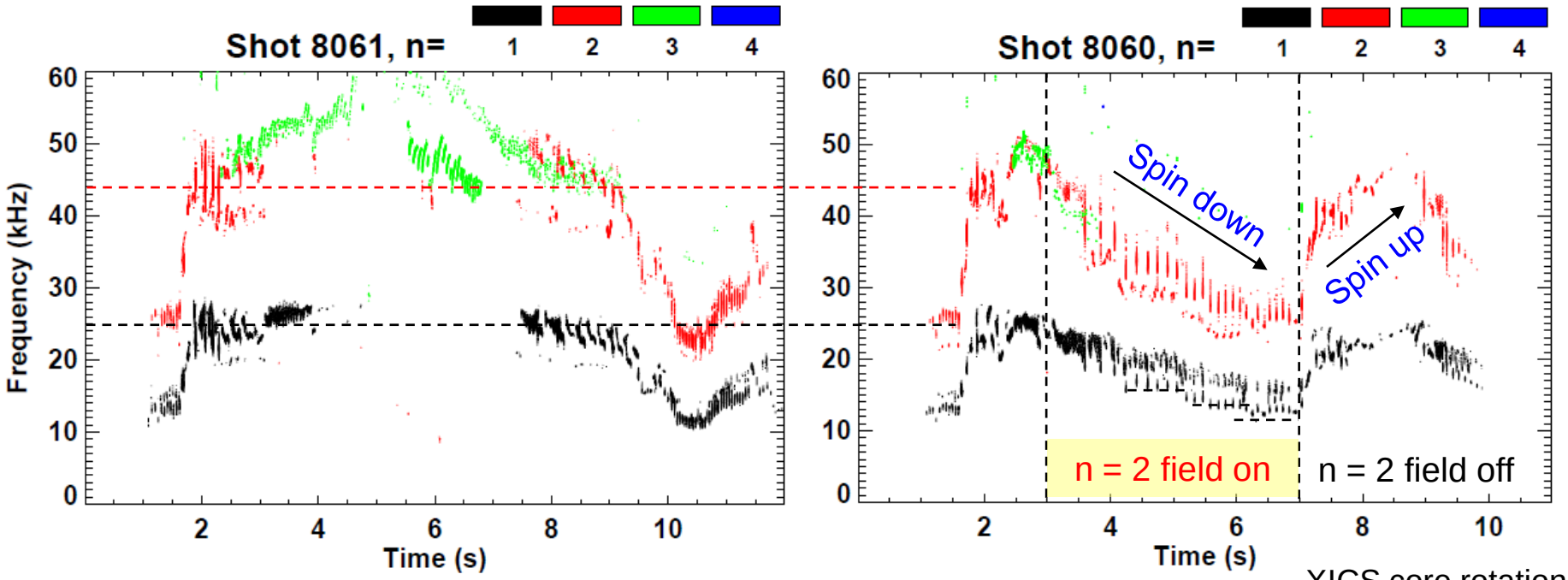

XICS core rotation

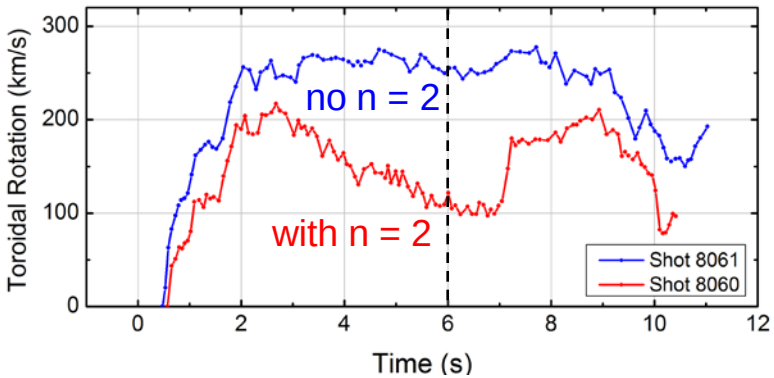

- Low frequency MHD mode rotation frequency decreased by 40 - 50% without mode locking
- Measureable energy confinement time change with n = 2 field applied
  - τ_E = 120 ms (no n = 2) vs. 90 ms (with n = 2) at 6 s in shot 8061 & 8060

Clear reduction in CES measured toroidal plasma rotation profile with applied n = 2 field

With IVCC n = 2 field

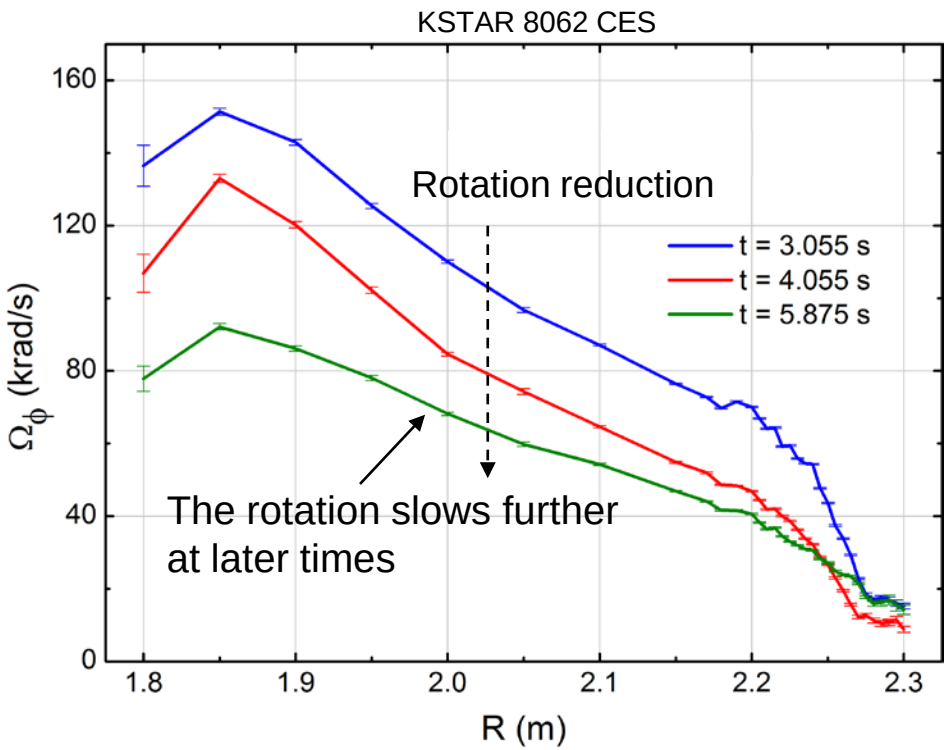

No IVCC n > 0 field

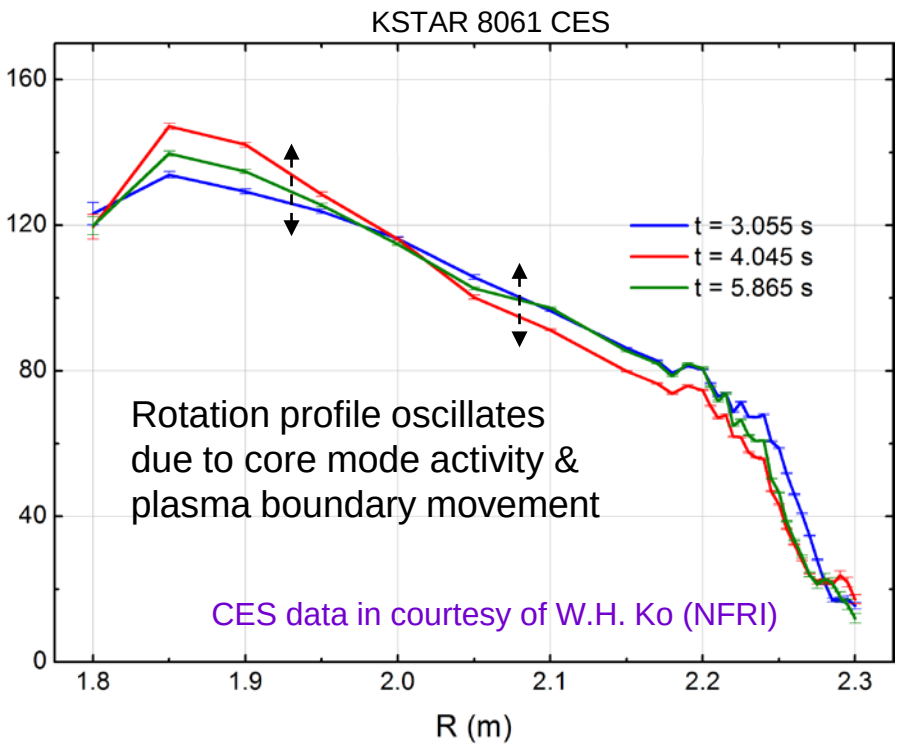

- Significant reduction of rotation speed using middle IVCC coil alone
- Significant alteration in rotation pedestal at the edge during braking
  - Slowed rotation profile resembles an L-mode profile (H-mode is maintained)

    → Edge rotation reduces first by NTV, then the core follows due to momentum diffusion